AJNR

MR Imaging Findings of Carcinoma Ex Pleomorphic Adenoma Related to Extracapsular Invasion and Prognosis

A. Akutsu, T. Horikoshi, H. Yokota, T. Wada, K. Motoori, K. Nasu, K. Yamasaki, T. Hanazawa, J.-I. Ikeda and T. Uno

AJNR Am J Neuroradiol 2022, 43 (11) 1639-1645
doi: https://doi.org/10.3174/ajnr.A7656
http://www.ajnr.org/content/43/11/1639

MR Imaging Findings of Carcinoma Ex Pleomorphic Adenoma Related to Extracapsular Invasion and Prognosis

A. Akutsu, T. Horikoshi, H. Yokota, T. Wada, K. Motoori, K. Nasu, K. Yamasaki, T. Hanazawa, J.-I. Ikeda, and T. Uno

ABSTRACT

BACKGROUND AND PURPOSE: MR imaging can reflect the pathologic progression of carcinoma ex pleomorphic adenoma (CXPA). This study aimed to identify the imaging findings related to extracapsular invasion of CXPA. Additionally, the pathologic background of these findings was investigated.

MATERIALS AND METHODS: This retrospective study included 37 patients with histologically confirmed CXPA. Three radiologists independently evaluated whether the CXPA showed the following characteristic MR imaging findings: border, capsule, the corona sign on fat-saturated T2WI and contrast-enhanced fat-saturated T1WI, and the black ring sign. The corona sign appeared larger on fat-saturated and/or contrast-enhanced fat-saturated T1WI than on T1WI. The black ring sign was defined as an intratumoral nodule with a thick low-intensity rim on T2WI. Interreader agreement of the visual assessment was performed using κ analysis, and MR imaging and histopathologic findings were also correlated. Kaplan-Meier survival and the log-rank test were used to estimate the 3-year disease-free survival.

RESULTS: MR imaging findings, especially peritumoral findings, showed a significant difference between invasive and noninvasive CXPA. The reliability was poor for the border and capsule. In contrast, it was good for the corona sign on fat-saturated and contrast-enhanced fat-saturated T1WI and the black ring sign. Pathologically, the corona sign reflected the invasiveness of the tumor and inflammatory cells, while the black ring sign reflected hyalinization or fibrosis. The corona sign also showed a significant difference in the 3-year disease-free survival.

CONCLUSIONS: MR imaging findings, including the corona and black ring signs, reliably differentiated invasive and noninvasive CXPA. The corona sign can be used as a prognostic factor for CXPA.

ABBREVIATIONS: CE = contrast-enhanced; CXPA = carcinoma ex pleomorphic adenoma; FS = fat-saturated; PA = pleomorphic adenoma

Carcinoma ex pleomorphic adenoma (CXPA) arises from a pre-existing pleomorphic adenoma (PA). It is more likely to occur in cases of PA with multiple recurrences or requiring long-term follow-ups. CXPA comprises 3.6% and 11.6% of all salivary gland tumors and malignancies, respectively, and is most often found in the parotid gland.[1,2]

Carcinoma in PA develops in the luminal cells of the tubular structures, and the malignant cells then destroy the pre-existing PA structure.[3-5] CXPA is classified by the World Health Organization as noninvasive, minimally invasive, or frankly invasive.[6] In CXPA, the carcinoma is considered noninvasive if the malignant cells are confined within the pre-existing PA capsule and invasive if the malignant cells cross over the capsule.[6,7] Noninvasive and minimally invasive CXPAs have a better prognoses and can be treated with localized resection. In contrast, frankly invasive CXPAs have a poor prognosis and require widespread resection, including the margins around the tumor.[6-8]

We hypothesized that MR imaging findings could reflect this pathologic spectrum of CXPA. CXPA may initially resemble PA, and the imaging findings are likely to change according to the pathologic changes that occur with carcinomatous invasion. The internal components of CXPA can show various imaging findings, depending on the proportions of the mucinous stroma and hyalinization/fibrosis proportions in the pre-existing PA and the histologic diversity of the carcinoma component.[9,10] Hence, we predicted that the imaging features of CXPA could be captured by focusing on the tumor margins rather than on its internal morphology.

Received March 11, 2022; accepted after revision August 19.

From the Department of Radiology (A.A., T.H., T.W., K.N.), Chiba University Hospital, Chiba, Japan; Diagnostic Radiology and Radiation Oncology (H.Y., T.U.) and Departments of Diagnostic Pathology (J.-I.I.) and Otorhinolaryngology, Head and Neck Surgery (K.Y., T.H.), Chiba University Graduate School of Medicine, Chiba, Japan; and Department of Radiology (K.M.), Tsudanuma Central General Hospital, Chiba Narashino-shi Yatsu, Japan.

Please address correspondence to Takuro Horikoshi, MD, Department of Radiology, Chiba University Hospital, 1-8-1, Inohana, Chuo-ku, Chiba, Chiba, 260-8677, Japan; e-mail: horikoshi@chiba-u.jp

Indicates article with online supplemental data.

http://dx.doi.org/10.3174/ajnr.A7656

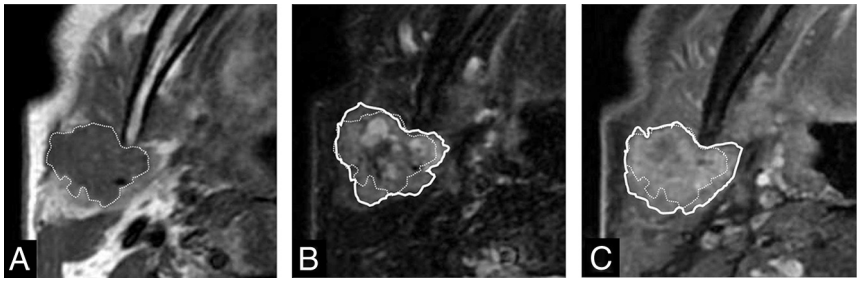

FIG 1. Corona sign on FS-T2WI and CE-FS-T1WI. Invasive CXPA (salivary duct carcinoma) of the right parotid gland in a 77-year-old man. MRI shows a homogeneous low-intensity tumor on axial T1WI (*A*), mixed high- and low-intensity signals on axial FS-T2WI (*B*), and irregularly enhanced signal on axial CE-FS-T1WI (*C*). The tumor size on FS-T2WI and CE-FS-T1WI (*solid line*) was larger than that on T1WI (*dotted line*). We defined these MRI findings as corona signs on FS-T2WI and CE-FS-T1WI.

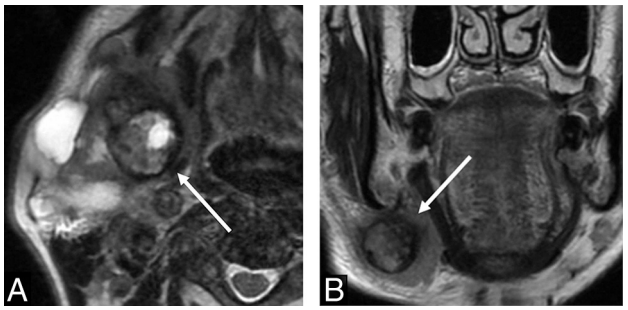

FIG 2. Black ring sign. Invasive CXPA (high-grade mucoepidermoid carcinoma) of the right submandibular gland in a 76-year-old man. MRI shows a nodule with a thick low-intensity rim (*A* and *B*, *arrows*) and an intra-ring component with mixed high- and low-intensity signals on axial and coronal T2WI (*A* and *B*). We defined this MRI finding as the black ring sign.

Only a few case reports describing the radiologic features of CXPA have been published. A previous review showed encapsulated components with a hypointense rim on T2WI and fat-saturated (FS) T2WI in some CXPA cases, which may be a characteristic finding.[3] However, the clinical significance of this finding has not been fully investigated.

Thus, we aimed to reveal the imaging spectrum of CXPA, specifically focusing on the imaging findings reflecting invasion beyond the PA capsule. In addition, we correlated the imaging findings with the pathologic background and subsequently evaluated the contribution of the imaging findings to prognosis.

MATERIALS AND METHODS

Study Participants

This retrospective study was approved by Chiba University Hospital review board, and the need for written informed consent was waived.

We found 41 potentially relevant cases via a computer search of the pathologic records between August 2007 and April 2020 at Chiba University Hospital. The following keyword phrase was used during the search: "carcinoma ex pleomorphic adenoma."

Patients were excluded for the following reasons: 1) absent or inaccessible MR images because the MR imaging was performed about 15 years ago ($n = 1$), 2) no head and neck MR imaging because of CXPA metastasis to the vertebral body ($n = 1$), 3) nonstandard MR imaging protocol (only intracranial MR imaging) ($n = 1$), and 4) lack of surgical-pathologic confirmation ($n = 1$). Of the 41 potential cases that were reviewed, only 37 patients who underwent an operation and had histopathologically proved CXPA were included. Five patients were aware of the mass for about 10 years but had neglected it. Six were under observation because of benign or suspected PA on fine-needle aspiration and imaging tests, and in 1 patient the tumor was surgically removed in the past. The patients underwent multiple preoperative imaging studies at various time points as part of their standard care.

In our institution, all patients underwent an initial CT examination approximately 3 months after the operation, followed by CT evaluations every 6 months. If recurrence was suspected, additional imaging studies, such as MR imaging and FDG-PET/CT or biopsies were performed. Patients who were pathologically positive or those with close surgical margins and who were histologically identified as having a high-grade malignancy also underwent postoperative radiation (60 Gy/30 fractions).

MR Imaging Protocol

MR images were obtained using a 1.5T scanner (Signa HDxt; GE Healthcare). The imaging protocol included axial T1WI, T2WI, FS-T2WI, and coronal T2WI sequences. Dynamic MR imaging, contrast-enhanced (CE)-FS-T1WI, and DWI/ADC mapping were also performed.

Image and Data Analysis

Clinical and prognostic data were extracted from the medical records, and MR imaging findings were independently evaluated by 3 radiologists with 6, 10, and 18 years of imaging experience, respectively. In cases involving initial disagreement, the final evaluation was decided by consensus among the 3 raters. Visual assessment of the tumor margins included the border and capsule. The border was evaluated using only conventional T1WI and T2WI, and the capsule was defined as the low-signal area and/or the contrast-effect area of the margin, in consideration of the chemical shift artifacts. The border was evaluated first, followed by the capsule. The border was assessed as well-defined, partially ill-defined, or totally ill-defined, and the capsule was assessed as complete, incomplete, or absent on a 3-point scale.

In addition, the corona signs on FS-T2WI and CE-FS-T1WI and the black ring sign were evaluated. The corona sign was considered if the tumor size on FS-T2WI or CE-FS-T1WI was larger than that on T1WI (Fig 1 and Online Supplemental Data). We defined the presence of a component encapsulated with a hypointense rim on T2WI or FS-T2WI as the black ring sign, as reported by Kashiwagi et al[3] (Fig 2). In this study, a lesion with a hypointense rim, which was noticeably thicker than the pre-existing PA capsule, was defined as the black ring sign. Intra-ring signals were not

Table 1: Clinical characteristics of CXPA

	Total	Invasive	Noninvasive	*P* Value
Age (mean) (yr)	64.7 (SD, 13.4)	65.7 (SD, 12.4)	62.7 (SD, 15.3)	.30
Sex				
Male	26	19	7	.44
Female	11	6	5	
Location				
Parotid gland	25	16	9	.68
Submandibular	7	6	1	
Minor salivary	5	3	2	
Laterality				
Left	17	9	8	.16
Right	20	16	4	
Swelling				
Yes	32	20	12	.15
No	5	5	0	
Pain				
Yes	13	10	3	.48
No	24	15	9	
Infection				
Yes	2	2	0	1
No	35	23	12	
Immobility				
Yes	12	10	2	.26
No	25	15	10	
Nerve palsy				
Yes	6	6	0	.15
No	31	19	12	
Skin infiltration				
Yes	1	1	0	1
No	36	24	12	

Table 2: Pathologic characteristics of CXPA

Pathology	Total	Invasive	Noninvasive	*P* Value
Salivary duct	18	11	7	.53
Myoepithelial	6	5	1	
Adenocarcinoma	3	3	0	
Squamous	3	1	2	
Mucoepidermoid	2	2	0	
Undifferentiated	1	1	0	
Unknown	4	2	2	

considered. Because the thickness of the PA capsule ranged from 15 to 1750 μm, we defined lesions with >2 mm thickness as having the black ring sign.[8]

Radiology-Pathology Correlation

Radiology-pathology correlation was assessed by 2 of the 3 radiologists who performed the imaging evaluations and a pathologist. The review was done with a consensus among these 3 individuals. In particular, we focused on peritumoral findings and the region corresponding to the black ring sign.

Statistical Analyses

We sorted the raters' findings into 2 groups for statistical analyses. Specifically, noninvasive and minimally invasive CXPAs were categorized into the noninvasive group, and frankly invasive CXPAs were categorized into the invasive group. For each imaging assessment, the Fisher exact probability test was performed in both the invasive and noninvasive groups. Interreader agreement of the visual assessment was performed using κ analysis. κ values were interpreted as follows: <0.40, poor to fair agreement; 0.41–0.60, moderate agreement; 0.61–0.80, substantial agreement; and 0.81–1.00, almost perfect agreement.[11] Kaplan-Meier survival and the log-rank test were used to estimate the 3-year disease-free survival. All statistical analyses were performed using R (Version 3.6.3; http://www.r-project.org/), and statistical significance was set at $P < .05$.

RESULTS

Clinical Findings

Two of the 37 patients were excluded from the CE image analysis because they had not undergone CE MR imaging. Twelve patients had noninvasive tumors, 25 with frankly invasive and 0 with minimally invasive tumors. The clinical characteristics of the patients are summarized in Table 1. Clinical information, such as age, sex, location, laterality, swelling, pain, infection, immobility, nerve palsy, and skin infiltration, showed no significant difference in relation to extracapsular invasion.

Pathologic Findings

The pathologic characteristics of the patients are summarized in Table 2. No significant difference was observed in the extracapsular invasion based on the histologic subtypes of the carcinoma.

MR Imaging Findings

The MR imaging findings of the border, capsule, corona sign on FS-T2WI and CE-FS-T1WI, and the black ring sign were significantly different in the 2 groups (Table 3). In the noninvasive group, the black ring sign was not observed in 11 of the 12 patients (91.7%). The black ring sign was observed with massive calcification of the left buccal region on CT in 1 case of maxillary CXPA; the calcification showed no signal on MR imaging and was mistakenly judged as the black ring sign.

Interrater Reliability

The κ values among the 3 raters are summarized in Table 4 and Online Supplemental Data. The border and capsule assessments showed poor agreement; in contrast, assessments of the corona signs on FS-T2WI and CE-FS-T1WI showed substantial agreement. Assessments of the black ring sign showed near-perfect agreement.

Radiology-Pathology Correlation

In the noninvasive group, the malignant component was completely surrounded by the fibrous capsule of the PA. Additionally, there was no infiltrating tumor or inflammatory cell infiltration into the normal salivary gland tissue beyond the lesion margins in this group (Fig 3).

In the invasive group, the corona signs on FS-T2WI and CE-FS-T1WI reflected tumor and/or inflammatory cells. The tumor

Table 3: Imaging findings of CXPA

	Total	Invasive	Noninvasive	*P* Value	OR 95% CI
Border					
Totally ill-defined	2	2	0	.002	14.41 (2.23–171.2)[a]
Partially ill-defined	19	17	2		
Well-defined	16	6	10		
Capsule					
None	9	9	0	<.001	38.18 (4.06–1956.7)[b]
Partial	12	11	1		
Total	16	5	11		
Corona sign on FS-T2WI					
Present	21	19	2	.001	14.40 (2.23–171.2)
Absent	16	6	10		
Corona sign on CE-FS-T1WI[c]					
Present	22	19	3	.007	9.31 (1.55–76.4)
Absent	13	5	8		
Black ring sign					
Present	15	14	1	.011	13.11 (1.49–642.2)
Absent	22	11	11		

[a] These ORs and 95% CIs were calculated between the 2 groups as well-defined versus totally ill-defined and partially ill-defined.
[b] These ORs and 95% CIs were calculated between the 2 groups as none and partial versus total.
[c] Two cases lacked contrast-enhanced images.

Table 4: Interrater reliability of visual assessment (κ value)[a]

	Rater 1 vs 2	Rater 1 vs 3	Rater 2 vs 3
Border	0.12	0.10	0.45
Capsule	0.19	0.38	0.16
Corona sign on FS-T2WI	0.78	0.79	0.67
Corona sign on CE-FS-T1WI	0.65	0.78	0.65
Black ring sign	0.89	0.84	0.84

[a] Raters 1, 2, and 3 had 6, 10, and 18 years of experience, respectively.

or inflammatory cells or both showed infiltration into the surrounding fatty tissue or salivary gland tissue. The black ring sign reflected hyalinization/fibrosis. Intra-ring components showed various cells and tissues (eg, carcinoma cells; hyalinization/fibrosis; comedonecrosis; and epithelial, myoepithelial, and mesenchymal components) containing mucoid, myxoid, and chondroid areas. These intra-ring components had diverse ratios of mucoid, myxoid, and chondroid stroma, depending on the individual case (Fig 4). Additionally, some PA components were present outside the black ring sign.

Prognosis

Significant differences were observed in the disease-free survival for invasiveness (Fig 5*A*, $P = .002$). Imaging findings showed significant differences in the corona signs on FS-T2WI and CE-T1WI. However, no difference was observed in the black ring sign (Fig 5*B*, *-D*, corona signs on FS-T2WI and CE-FS-T1WI [$P < .001$ and $P = .001$, respectively] and black ring sign [$P = .31$]).

DISCUSSION

The current study yielded 3 main findings: First, the imaging findings (the border, capsule, corona signs on FS-T2WI and CE-FS-T1WI, and black ring sign) were significantly different between the invasive and noninvasive groups. These differences were useful for distinguishing invasiveness beyond the ex-PA capsule. Second, the corona signs on FS-T2WI and CE-FS-T1WI reflected the presence of an extracapsular tumor and/or inflammatory cells. For the black ring sign, the hypointense rim on T2WI or FS-T2WI indicated hyalinization/fibrosis, and the intra-ring components reflected various cells and tissues pathologically. Third, a significant difference in disease-free survival was observed between the invasive and noninvasive groups, and pathologic extracapsular invasion was confirmed to be a prognostic factor. In addition, the imaging findings of the corona signs on FS-T2WI and CE-FS-T1WI were also prognostic factors.

To the best of our knowledge, this study included the largest number of CXPAs and is the first to compare the imaging findings of CXPA based on the World Health Organization's classification of invasiveness. Surgical resection is the first choice of treatment for CXPA. Partial lobectomy is indicated for noninvasive or minimally invasive CXPAs localized in the superficial lobe of the parotid gland, and total parotidectomy is indicated for frankly invasive CXPA.[12] Preoperative MR imaging may facilitate surgical planning and prognosis when one is seeking to manage CXPA.

Marginal information could be used to differentiate invasive and noninvasive CXPAs. We considered that a fibrous capsule usually surrounds a PA and that the appearance of invasion beyond the capsule affects the morphology of the capsule and border. However, the interrater reliability was poor for border and capsule findings. This poor reliability might be due to variations in the pre-existing PA. PA can present with a lobulated morphology, and even a normal PA can have an incomplete capsule or no capsule. In PA of minor salivary glands, the capsule surrounding the lobules could be unclear or missing.[13,14] In addition, chemical shift artifacts make it difficult to assess thin capsules. Conversely, the corona signs on FS-T2WI and CE-FS-T1WI and the black ring sign showed good interrater reliability (Table 4). These findings may be useful for assessing marginal findings.

The corona signs on FS-T2WI and CE-FS-T1WI reflected pathologically extracapsular tumor and/or inflammatory cells, which could indicate invasion. The black ring sign was a highly specific finding (Table 3; specificity, 91.7% [11 of 12 patients]) for invasive CXPA, with 1 case in which massive calcification was mistaken for a black ring sign. Calcification can be easily recognized on CT images, and its specificity may increase further. In the pathologic evaluation, severe hyalinization and fibrosis were observed, which manifested as a hypointense rim of the black ring sign on T2WI or FS-T2WI. On MR imaging, the intra-ring components of the black ring sign showed various signals.

Pathologically, various components, such as hyaline, mucoid, myxoid, and chondroid stroma, were present, and the proportions of these components varied in each case. The organization of PA shows various patterns and a wide range of morphologic and structural diversity.[13,14] The black ring sign is suggested to reflect a pre-existing PA or a part of the existing PA. Extensive hyalinization or fibrosis has been identified as an important predictor of malignant transformation in PAs in several pathologic studies. This finding supports our hypothesis,[15-17] and we observed that the black ring sign effectively assessed invasiveness. If the black ring sign reflects a pre-existing PA, it could be a sign of invasive CXPA.

In the survival curve, pathologic invasion beyond the pre-existing PA capsule was associated with recurrence. This result was consistent with previous reports, and CXPA without extracapsular infiltration showed benign behavior.[15,18-21] Our results showing no recurrence in noninvasive cases were similar to those reported by Mariano et al[18] and Zhao et al.[19] Therefore, noninvasive CXPA may be managed surgically, similar to benign PAs.

Information on the tumor margins, such as the corona signs on FS-T2WI and CE-FS-T1WI, was a prognostic finding. The black ring sign did not show a significant difference in prognosis. This finding is because the black ring sign had high specificity but low sensitivity to extracapsular infiltration of the CXPA (Table 3; sensitivity, 56% [14 of 25 patients]).

This study had some limitations. First, the histologic types of the carcinomas in the CXPA varied in our study, and this variation may have affected the imaging findings. Second, only CXPA—and no other type of salivary gland tumor—was studied. Third, although CXPA has been classified into 3 types based on the degree of invasiveness, this study did not include cases of minimally invasive CXPA. Minimally invasive CXPA may be overlooked because it requires pathologic evaluation of all tumor margins. However, none of the cases that were actually considered noninvasive showed recurrence, and the prognosis was clearly divided between invasive and noninvasive cases. These findings indicate that a proper pathologic classification was performed.

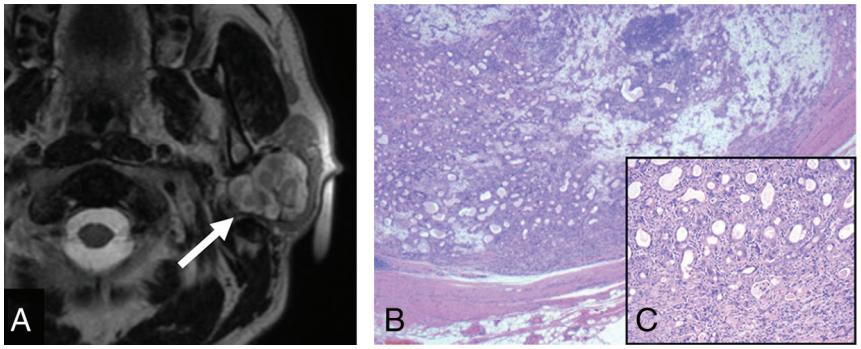

FIG 3. MR imaging–pathology correlation: noninvasive type. Noninvasive CXPA (salivary duct carcinoma) of the left parotid gland in a 56-year-old man. MRI showed a heterogeneous high-intensity tumor on axial T2WI (*A, arrow*). The corona signs on FS-T2WI and CE-FS-T1WI and the black ring sign were absent. Photomicrograph shows ductal and myoepithelial cells in the chondromyxoid stroma. A part of the tumor contained ductal and myoepithelial cells with atypical hyperchromatic nuclei. The malignant component was completely surrounded by the fibrous capsule of the pre-existing pleomorphic adenoma (*B*, H&E, original magnification ×20). Note higher magnification of the malignant component (*C*, H&E, original magnification ×100).

CONCLUSIONS

MR imaging is useful for differentiating invasive and noninvasive CXPAs. The corona signs on FS-T2WI and CE-FS-T1WI were reliable predictors of the invasiveness of CXPA and overall prognosis. The black ring sign was also a characteristic feature of invasive CXPA. Distinction between invasive

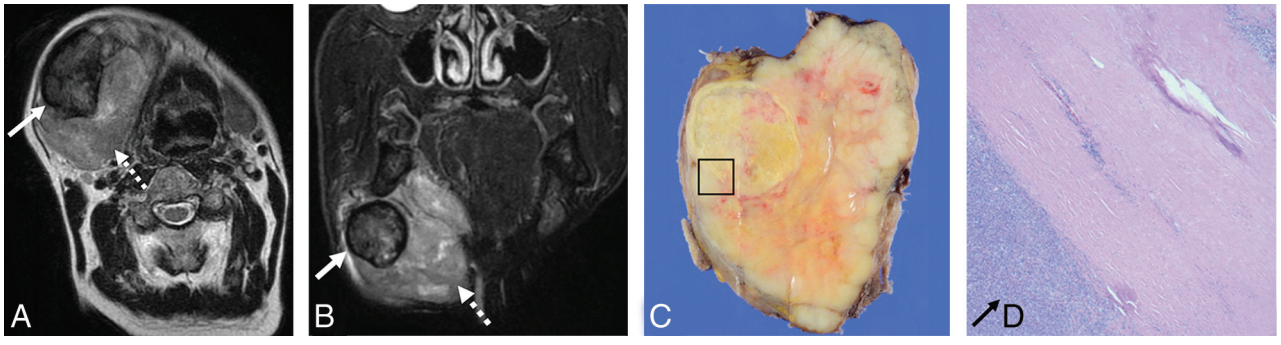

FIG 4. MR imaging–pathology correlation: invasive type. Invasive CXPA (undifferentiated carcinoma, large-cell type) of the right submandibular gland in a 72-year-old man. A huge mass replaced the right submandibular gland. MRI shows heterogeneous high intensity on T2WI and FS-T2WI (*A* and *B*, *dotted arrows*). Encapsulated nodules with thick low-intensity rims are present inside the tumor on axial T2WI and FS-T2WI (*A* and *B*, *solid arrows*). Macroscopic findings show a solid and white-yellow tumor with nodules in the nodule pattern. The nodule within the tumor corresponds to a black ring sign on MRI (*C*). Photomicrograph shows ductal and myoepithelial cells with atypical hyperchromatic nuclei (*D*, H&E, original magnification ×20). The malignant component invaded beyond the capsule (*D, arrows*) and infiltrated the surrounding fatty tissue. Most nodules within the tumor showed extensive hyalinization/fibrosis with myxoid stroma (*D*), and the black ring sign matched the hyalinization/fibrosis. The corona sign on FS-T2WI and CE-FS-T1WI reflects pathologically extracapsular tumor cells and/or inflammatory cells.

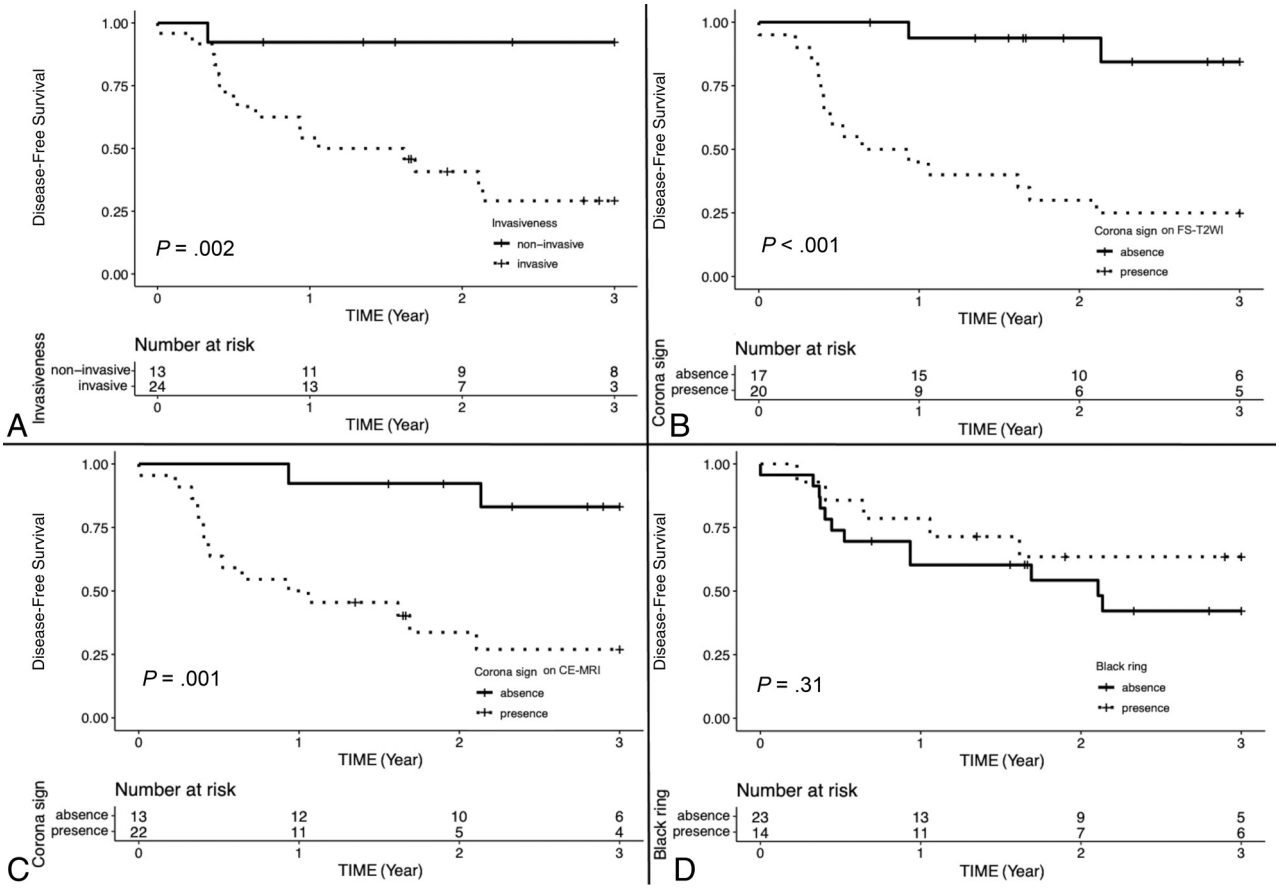

FIG 5. Kaplan-Meier disease-free survival curves and number-at-risk table of invasiveness (*A*), corona signs on FS-T2WI and CE-FS-TIWI (*B* and *C*), and the black ring sign (*D*).

and noninvasive CXPAs using preoperative MR imaging may contribute to surgical planning and prediction of the prognosis of CXPA.

Disclosure forms provided by the authors are available with the full text and PDF of this article at www.ajnr.org.

REFERENCES

1. Gnepp DR. **Malignant mixed tumours of the salivary glands: a review.** *Pathol Annu* 1993;28:279–328 Medline
2. Olsen KD, Lewis JE. **Carcinoma ex pleomorphic adenoma: a clinicopathologic review.** *Head Neck* 2001;23:705–12 CrossRef Medline
3. Kashiwagi N, Murakami T, Chikugo T, et al. **Carcinoma ex pleomorphic adenoma of the parotid gland.** *Acta Radiol* 2012;53:303–06 CrossRef Medline
4. Kato H, Kanematsu M, Mizuta K, et al. **Carcinoma ex pleomorphic adenoma of the parotid gland; radiopathologic correlation with MR imaging including diffusion-weighted imaging.** *AJNR Am J Neuroradiol* 2008;29:865–67 CrossRef Medline
5. Weiler C, Zengel P, van der Wal JE, et al. **Carcinoma ex pleomorphic adenoma with special reference to the prognostic significance of histological progression: a clinicopathological investigation of 41 cases.** *Histopathology* 2011;59:741–50 CrossRef Medline
6. El-Naggar AK, Chan JK, Grandis JR, et al. *World Health Organization Classification of Tumours: Pathology and Genetics of Head and Neck Tumours*. 4th ed. International Agency for Research on Cancer; 2017
7. Guzzo M, Locati LD, Prott FJ, et al. **Major and minor salivary gland tumors.** *Crit Rev Oncol Hematol* 2010;74:134–48 CrossRef Medline
8. Webb AJ, Eveson JW. **Pleomorphic adenomas of the major salivary glands: a study of the capsular form in relation to surgical management.** *Clin Otolaryngol Allied Sci* 2001;26:134–42 CrossRef Medline
9. Klijanienko J, El-Naggar AK, Vielh P. **Fine-needle sampling findings in 26 carcinoma ex pleomorphic adenomas: diagnostic pitfalls and clinical considerations.** *Diagn Cytopathol* 1999;21:163–66 CrossRef Medline
10. Wada T, Yokota H, Horikoshi T, et al. **Diagnostic performance and inter-operator variability of apparent diffusion coefficient analysis for differentiating pleomorphic adenoma and carcinoma ex pleomorphic adenoma: comparing one-point measurement and whole-tumor measurement including radiomics approach.** *Jpn J Radiol* 2020;38:207–14 CrossRef Medline
11. Landis JR, Koch GG. **The measurement of observer agreement for categorical data.** *Biometrics* 1977;33:159–74 CrossRef Medline
12. Antony J, Gopalan V, Smith RA, et al. **Carcinoma ex pleomorphic adenoma: a comprehensive review of clinical, pathological and molecular data.** *Head Neck Pathol* 2012;6:1–9 CrossRef Medline
13. Mărgăritescu C, Raica M, Simionescu C, et al. **Tumoral stroma of salivary pleomorphic adenoma-histopathological, histochemical and immunohistochemical study.** *Rom J Morphol Embryol* 2005;46:211–23 Medline
14. de Sousa Lopes ML, Barroso KM, Henriques ÁC, et al. **Pleomorphic adenomas of the salivary glands: retrospective multicentric study of 130 cases with emphasis on histopathological features.** *Eur Arch Otorhinolaryngol* 2017;274:543–51 CrossRef Medline
15. Lewis JE, Olsen KD, Sebo TJ. **Carcinoma ex pleomorphic adenoma: pathologic analysis of 73 cases.** *Hum Pathol* 2001;32:596–604 CrossRef Medline

16. Auclair PL, Ellis GL. **Atypical features in salivary gland mixed tumors: their relationship to malignant transformation.** *Mod Pathol* 1996;9:652–67 [Database] Medline
17. Ethunandan M, Witton R, Hoffman G, et al. **Atypical features in pleomorphic adenoma–a clinico-pathologic study and implications for management.** *Int J Oral Maxillofac Surg* 2006;35:608–12 CrossRef Medline
18. Mariano FV, Noronha AL, Gondak RO, et al. **Carcinoma ex pleomorphic adenoma in a Brazilian population: clinico-pathological analysis of 38 cases.** *Int J Oral Maxillofac Surg* 2013;42:685–92 CrossRef Medline
19. Zhao J, Wang J, Yu C, et al. **Prognostic factors affecting the clinical outcome of carcinoma ex pleomorphic adenoma in the major salivary gland.** *World J Surg Onc* 2013;11:180 CrossRef Medline
20. Masahiro S, Takashi M, Satoshi S, et al. **Carcinoma ex pleomorphic adenoma of the parotid gland: a multi-institutional retrospective analysis in the Northern Japan Head and Neck Cancer Society.** *Acta Otolaryngol* 2016;136:1154–58 CrossRef Medline
21. Katabi N, Gomez D, Klimstra DS, et al. **Prognostic factors of recurrence in salivary carcinoma ex pleomorphic adenoma, with emphasis on the carcinoma histologic subtype: a clinicopathologic study of 43 cases.** *Hum Pathol* 2010;41:927–34 CrossRef Medline